Article

Are the Radical Centers in Peptide Radical Cations Mobile? The Generation, Tautomerism, and Dissociation of Isomeric #-Carbon-Centered Triglycine Radical Cations in the Gas Phase

Ivan K. Chu, Junfang Zhao, Minjie Xu, Shiu On Siu, Alan C. Hopkinson, and K. W. Michael Siu

J. Am. Chem. Soc., **2008**, 130 (25), 7862-7872 • DOI: 10.1021/ja801108j • Publication Date (Web): 31 May 2008

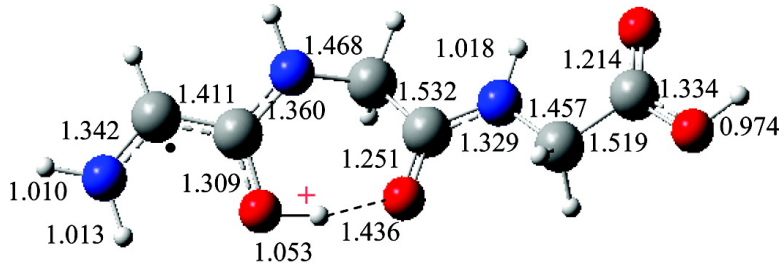

$[G^{\bullet}GG]^{+}$ at global minimum

More About This Article

Additional resources and features associated with this article are available within the HTML version:

- Supporting Information
- Links to the 1 articles that cite this article, as of the time of this article download
- Access to high resolution figures
- Links to articles and content related to this article
- Copyright permission to reproduce figures and/or text from this article

View the Full Text HTML

J|A|C|S
ARTICLES

Published on Web 05/31/2008

Are the Radical Centers in Peptide Radical Cations Mobile? The Generation, Tautomerism, and Dissociation of Isomeric α-Carbon-Centered Triglycine Radical Cations in the Gas Phase

Ivan K. Chu,*,† Junfang Zhao,‡ Minjie Xu,† Shiu On Siu,† Alan C. Hopkinson,‡ and K. W. Michael Siu*,‡

Department of Chemistry, University of Hong Kong, Pokfulam Road, Hong Kong, China and Department of Chemistry and Centre for Research in Mass Spectrometry, York University, 4700 Keele Street, Toronto, Ontario, Canada M3J 1P3

Received February 13, 2008; E-mail: ivankchu@hkucc.hku.hk; kwmsiu@yorku.ca

Abstract: The mobility of the radical center in three isomeric triglycine radical cations—$[G^{\bullet}GG]^+$, $[GG^{\bullet}G]^+$, and $[GGG^{\bullet}]^+$—has been investigated theoretically via density functional theory (DFT) and experimentally via tandem mass spectrometry. These radical cations were generated by collision-induced dissociations (CIDs) of Cu(II)-containing ternary complexes that contain the tripeptides YGG, GYG, and GGY, respectively (G and Y are the glycine and tyrosine residues, respectively). Dissociative electron transfer within the complexes led to observation of $[Y^{\bullet}GG]^+$, $[GY^{\bullet}G]^+$, and $[GGY^{\bullet}]^+$; CID resulted in cleavage of the tyrosine side chain as *p*-quinomethide, yielding $[G^{\bullet}GG]^+$, $[GG^{\bullet}G]^+$, and $[GGG^{\bullet}]^+$, respectively. Interconversions between these isomeric triglycine radical cations have relatively high barriers (≥44.7 kcal/mol), in support of the thesis that isomerically pure $[G^{\bullet}GG]^+$, $[GG^{\bullet}G]^+$, and $[GGG^{\bullet}]^+$ can be experimentally produced. This is to be contrasted with barriers < 17 kcal/mol that were encountered in the tautomerism of protonated triglycine [Rodriquez C. F. et al. *J. Am. Chem. Soc.* **2001**, *123*, 3006−3012]. The CID spectra of $[G^{\bullet}GG]^+$, $[GG^{\bullet}G]^+$, and $[GGG^{\bullet}]^+$ were substantially different, providing experimental proof that initially these ions have distinct structures. DFT calculations showed that direct dissociations are competitive with interconversions followed by dissociation.

1. Introduction

Ionizing radiation and oxidizing agents both cause extensive damage to amino acids and peptides through formation of radicals; understanding how these radicals are formed and how they react is, therefore, of great importance.[1–3] A number of novel approaches have emerged for the production of large radical cations of biomolecules, and more than 10 recent studies have examined the dissociations of odd-electron radical peptide ions in the gas phase.[4–15] The fragmentation behavior of these radical ions has been found to be rich and fascinating, differing considerably from that of protonated peptides, and can provide complementary information that is potentially useful for peptide sequencing. In addition to applications in tandem mass spectrometry, the dissociation of radical cationic peptides has also been used for modeling molecular wires in studies of electrical conduction in biological systems[16] and for investigating intramolecular vibrational redistribution in unimolecular fragmentations.[17] The dissociation pathways of the α-carbon-centered radical $[DRVG^{\bullet}IHPF]^+$ under surface-induced dissociation have been described successfully using statistical (Rice−Ramsperger−Kassel−Marcus, RRKM) theory.[18] Previous investigations[6–15] have found that the location of the charge and hydrogen bonding play an important role in determining the observed product ions of peptides containing basic residues. The fragmentation pathways depend not only on the proton affinities of the residues but also on the location of the radical. Comprehensive studies on the roles of radical sites have, however, been hindered by difficulties in generating peptide radical cations with initial radical sites located at well-defined positions. The dissociations of radical cationic amino acids and tryptophan-containing tripeptides have been examined using both tandem mass spectrometry and density functional theory (DFT).[7] The fragmentations of tryptophan-containing radical tripeptides lead to a number of characteristic product ions, including $[a_n + H]^{\bullet+}$, $[z_n - H]^{\bullet+}$, and $[w_n + H]^{\bullet+}$, through cleavages of the $C_\alpha-C$ and $N-C_\alpha$ bonds and facile side-chain cleavage of the tryptophan residue.

† University of Hong Kong.
‡ York University.

(1) Stubbe, J.; van der Donk, W. A. *Chem. Rev.* **1998**, *98*, 705–762.
(2) Berlett, B. S.; Stadtman, E. R. *J. Biol. Chem.* **1997**, *272*, 20313–20316.
(3) Stadtman, E. R. *Annu. Rev. Biochem.* **1993**, *62*, 797–821.
(4) Rauk, A.; Yu, D.; Armstrong, D. A. *J. Am. Chem. Soc.* **1997**, *119*, 208–217.
(5) Barone, V.; Adamo, C.; Grand, A.; Jolibois, F.; Brunel, Y.; Subra, R. *J. Am. Chem. Soc.* **1995**, *117*, 12618–12624.
(6) Chu, I. K.; Rodriquez, C. F.; Lau, T.; Hopkinson, A. C.; Siu, K. W. M. *J. Phys. Chem. B* **2000**, *104*, 3393.
(7) Bagheri-Majdi, E.; Ke, Y.; Orlova, G.; Chu, I. K.; Hopkinson, A. C.; Siu, K. W. M. *J. Phys. Chem. B* **2004**, *108*, 11170–11181.
(8) Barlow, C. K.; Wee, S.; McFadyen, W. D.; O'Hair, R. A. J. *Dalton Trans.* **2004**, *20*, 3199–3204.
(9) Chu, I. K.; Rodriquez, C. F.; Hopkinson, A. C.; Siu, K. W. M. *J. Am. Soc., Mass Spectrom.* **2001**, *12*, 1114–1119.

10.1021/ja801108j CCC: $40.75

The calculated lowest-energy structure of the radical cation of triglycine is a captodative radical in which the α-carbon of the N-terminal residue is formally the radical center and is flanked by both a strongly electron-withdrawing group ($[-C(OH)NH]^+$) and a powerful electron donor (NH_2-), thereby imparting the radical with exceptional stability known as the captodative effect.[7,19]

The notion of charge-directed fragmentation through a "mobile proton" has been used to rationalize some of the dissociation pathways of aliphatic-only and tryptophan-containing radical tripeptide ions. However, radical-driven dissociations are a distinct possibility for the other reactions. A recent comparison[20] of the dissociation patterns of time- and collision-energy-resolved SIDs of the $M^{\bullet+}$, $[M + H]^{\bullet 2+}$, and $[M - 2H]^{\bullet-}$ ions of model peptides with basic amino acid residues provided clear evidence that charge-remote, radical-induced fragmentations play a critical role during the dissociation of odd-electron peptide ions, particularly with respect to side-chain losses and some peptide backbone cleavages. The competitive radical- and mobile-proton-induced dissociations of radical peptides bound to alkali metal ions, including sodium and lithium ions, are metal-specific. O'Hair and co-workers[21,22] examined the gas-phase fragmentation chemistries of fixed-charge peptide radicals. By using an "inert" fixed charge positioned at a well-defined location, the fragmentation of the peptide was restricted to radical-driven processes, and competing charge-directed processes were minimized. O'Hair and co-workers suggested that multiple 1,4-hydrogen atom migrations, including those from the N-terminus to the C-terminus, occur in larger peptides. By contrast, Wesdemiotis and co-workers[23] reported that the lithiated and dilithiated radical cationic isomers of dipeptides are not interconvertible. Turecek and Syrstad[24] investigated radical peptide rearrangements and intramolecular hydrogen-atom migrations using *N*-methylacetamide and *β*-alanine as models; they found that the migration of an ammonium H-atom is competitive with its elimination.

Here, we report an examination of the three α-carbon-centered radical cations of the simplest tripeptide, triglycine. The lower-energy structures of each of the radical cations—$[G^{\bullet}GG]^+$, $[GG^{\bullet}G]^+$, and $[GGG^{\bullet}]^+$—and the barriers against interconversions were determined using DFT. (The residue to the left of the • contains the radical site; in each triglycine the α-carbon has the highest spin; the location of the charge is less well-defined as the proton is typically hydrogen-bonded, resulting in charge delocalization.) Experimentally, these radical cations were generated through multiple stages of collision-induced dissociation (CID) of $[Cu^{II}(L)(M)]^{\bullet 2+}$ complexes (where L = auxiliary ligand and M = YGG, GYG, or GGY; Y and G are the tyrosine and glycine residues, respectively). Dissociative electron transfer within these complexes results in $[Cu^{I}(L)]^+$ and $M^{\bullet+} = [Y^{\bullet}GG]^+$, $[GY^{\bullet}G]^+$, and $[GGY^{\bullet}]^+$, respectively.[6,14] The three α-carbon-centered radical cations—$[G^{\bullet}GG]^+$, $[GG^{\bullet}G]^+$, and $[GGG^{\bullet}]^+$—each with a well-defined initial radical site were formed through $C_\alpha-C_\beta$ homolytic bond cleavages of the tyrosyl residues of, respectively, $[Y^{\bullet}GG]^+$, $[GY^{\bullet}G]^+$, and $[GGY^{\bullet}]^+$. The key objective of this study was to determine whether the radical center is "mobile" under experimental conditions, bearing in mind that the mobile proton theory is central to the rationalization of dissociations of protonated peptides.[25–27] The extreme case is that, if the radical site is very mobile, then this would result in very similar and even identical CID spectra from the three precursors ions, $[G^{\bullet}GG]^+$, $[GG^{\bullet}G]^+$, and $[GGG^{\bullet}]^+$. Interpretations and deductions were aided by DFT calculations on the energetics and structures of the three isomeric triglycine radical cations and the energy profiles to their interconversion and fragmentation reactions.

2. Experimental Section

2.1. Chemicals. All chemicals and reagents were commercially available (Sigma-Aldrich, St. Louis, MO; and Bachem, King of Prussia, PA). YGG, GYG, and GGY were synthesized according to a literature procedure.[28] Fmoc-protected amino acids and the Wang resin were purchased from Advanced ChemTech (Louisville, KY). Copper(II)-containing ternary complexes were prepared *in situ* by mixing copper(II) perchlorate hexahydrate with the crown ether 1,4,7,10-tetraoxacyclododecane (12-crown-4) or 4′-chloro-2,2′:6′,2″-terpyridine (4Cl-tpy) in a water/methanol solution (1:1).

2.2. Mass Spectrometry. Experiments were conducted using a quadrupole ion trap mass spectrometer (Finnigan LCQ, Thermo-Finnigan, San Jose, CA). Samples typically comprised 600 mM of the complex and 50 mM of the oligopeptide in a water/methanol (1:1) solution. A syringe pump (Cole Parmer, Vernon Hills, IL) was used for direct infusion of the electrospray samples at flow rates ranging from 30 to 50 μL/h. CID spectra were acquired using helium as the collision gas. The injection and activation times for

(10) O'Hair, R. A. J.; Blanksby, S.; Styles, M.; Bowie, J. H. *Int. J. Mass Spectrom.* **1999**, *182/183*, 203–211.
(11) Turecek, F.; Carpenter, F. H.; Polce, M. J.; Wesdemiotis, C. *J. Am. Chem. Soc.* **1999**, *121*, 7955–7956.
(12) Polce, M. J.; Wesdemiotis, C. *J. Am. Soc., Mass Spectrom.* **1999**, *10*, 1241–1247.
(13) Turecek, F.; Howland, C. F. *J. Chem. Soc., Perkin Trans. 2* **1999**, 2315–2323.
(14) Hopkinson, A. C.; Siu, K. W. M. In *Peptide Radical Cations in: Principles of Mass Spectrometry Applied to Biomolecules*; Laskin, J., Liftshitz, C., Eds.; John Wiley and Sons: NJ, 2006; pp 301−335.
(15) Chu, I. K.; Lam, C. N. W.; Siu, S. O. *J. Am. Soc. Mass Spectrom.* **2005**, *16*, 1795–1804.
(16) (a) Kemp, M.; Roiterg, A.; Mujica, V.; Wanta, T.; Ratner, M. A. *J. Phys. Chem.* **1996**, *100*, 8349–8355. (b) Schlag, E. W.; Lin, S. H.; Weinkauf, R.; Rentzepis, P. M. *Proc. Natl. Acad. Sci. U.S.A.* **1998**, *95*, 1358–1362.
(17) (a) Schlag, E. W.; Levine, R. D. *Chem. Phys. Lett.* **1989**, *163*, 523–530. (b) Hu, Y. J.; Hadas, B.; Davidovitz, M.; Balta, B.; Lifshitz, C. *J. Phys. Chem. A* **2003**, *107*, 6507–6514.
(18) Laskin, J.; Futrell, J. H.; Chu, I. K. *J. Am. Chem. Soc.* **2007**, *129*, 9598–9799.
(19) Zhao, J.; Siu, K. W. M.; Hopkinson, A. C. *Phys. Chem. Chem. Phys.* **2008**, *10*, 281–288.
(20) Laskin, J.; Yang, Z.; Lam, C.; Chu, I. K. *Anal. Chem.* **2007**, *79*, 6607–6614.
(21) Karnezis, A.; Barlow, C. K.; O'Hair, R. A. J.; McFadyen, W. D. *Rapid Commun. Mass Spectrom.* **2006**, *20*, 2865–2870.
(22) Wee, S.; Mortimer, A.; Moran, D.; Wright, A.; Barlow, C. K.; O'Hair, R. A. J.; Radom, L.; Easton, C. J. *Chem. Commun.* **2006**, 4233–4235.
(23) Pingitore, F.; Bleiholder, C.; Paizs, B.; Wesdemiotis, C. *Int. J. Mass Spectrom.* **2007**, *265*, 251–260.
(24) Turecek, F.; Syrstad, E. A. *J. Am. Chem. Soc.* **2003**, *125*, 3353–3369.
(25) (a) Jones, J. L.; Dongre, A. R.; Somogyi, A.; Wysocki, V. H. *J. Am. Chem. Soc.* **1994**, *116*, 8368–8369. (b) Dongre, A. R.; Jones, J. L.; Somogyi, A.; Wysocki, V. H. *J. Am. Chem. Soc.* **1996**, *118*, 8365–8374. (c) Dongre, A. R.; Somogyi, A.; Wysocki, V. H. *J. Mass Spectrom.* **1996**, *31*, 339–350.
(26) (a) Tsapralis, G.; Nair, H.; Somogyi, A.; Wysocki, V. H.; Zhong, W.; Futrell, J. H.; Summerfield, S. G.; Gaskell, S. J. *J. Am. Chem. Soc.* **1999**, *121*, 5142–5154. (b) Gu, C.; Somogyi, A.; Wysocki, V. H.; Medzihradsky, K. F. *Anal. Chim. Acta* **1999**, *397*, 247–256. (c) Harrison, A. G.; Yalcin, T. *Int. J. Mass Spectrom. Ion Processes* **1997**, *165−167*, 339–347. (d) Mueller, D. R.; Eckersley, M.; Richter, W. *Org. Mass Spectrom.* **1988**, *23*, 217–222. (e) Johnson, R. S.; Krylov, D.; Walsh, K. A. *J. Mass Spectrom.* **1995**, *30*, 368–387. (f) Vaisar, T.; Urban, J. *J. Mass Spectrom.* **1998**, *33*, 505–524.
(27) Rodriquez, C. F.; Cunje, A.; Shoeib, T.; Chu, I. K.; Hopkinson, A. C.; Siu, K. W. M. *J. Am. Chem. Soc.* **2001**, *123*, 3006–3012.
(28) Chan, W. C.; White, P. D. *Fmoc Solid Phase Peptide Synthesis: A Practical Approach*; Oxford: New York, 2000.

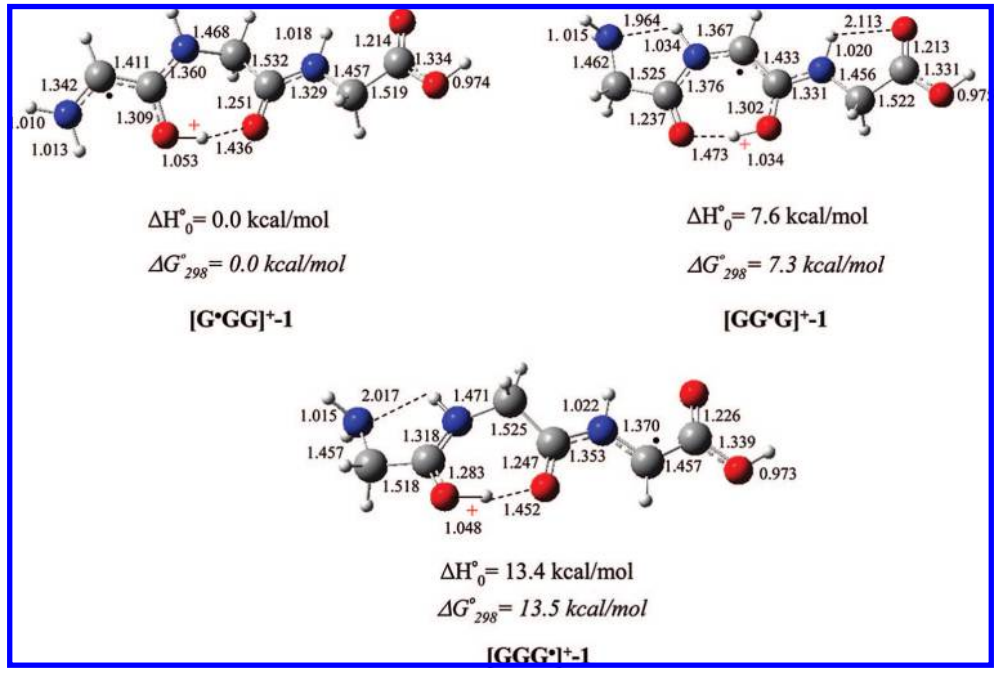

Figure 1. Optimized lowest-energy structures for $[G^{\bullet}GG]^{+}$, $[GG^{\bullet}G]^{+}$, and $[GGG^{\bullet}]^{+}$ (bond lengths, Å).

CID were 200 and 30 ms, respectively; the percent collision energy was optimized for each experiment. To record the product ion spectrum of a triglycine radical cation, for example $[G^{\bullet}GG]^{+}$, an MS^4 experiment involving sequential isolation of (1) $[Cu^{II}(4Cl\text{-}tpy)(YGG)]^{\bullet 2+}$, (2) $[Y^{\bullet}GG]^{+}$ and (3) $[G^{\bullet}GG]^{+}$, and finally CID of $[G^{\bullet}GG]^{+}$ was typically required. The fragmentation chemistries of the radical peptide ions thus generated were independent of the choice of 12-crown-4 or 4Cl-tpy as the auxiliary ligand.

2.3. Computational. All calculations were performed using the Gaussian 03 suite of programs[29] and the hybrid DFT UB3LYP method based on Becke's three-parameter exchange functional[30] and Lee, Yang, and Parr's correlation functional.[31] Geometries of the triglycine radical cations were fully optimized using the 6−31++G(d,p) basis set. Many of the reactions investigated involved multiple steps; for tractability, on the potential energy surfaces (PESs) we show only the critical transitions states and intermediates. Harmonic frequency calculations were performed to characterize each critical point and to determine zero-point vibrational energies. Each transition state structure for the isomerization and fragmentation reactions was shown to have only a single imaginary frequency. The reactants and products associated with each transition state structure were identified using the intrinsic reaction coordinate (IRC) method.[32]

Performance of the UB3LYP method was verified by the UBMK method.[33] Key minimum and transition structures obtained by UB3LYP/6−31++G(d,p) were reoptimized with UBMK/6−31++G(d,p). All structures and energies reported in this study, unless otherwise specified, are those obtained by UB3LYP/6−31++G(d,p). Details of the structures obtained by both methods are available as Supporting Information.

3. Results and Discussion

3.1. Low-Energy Structures of $[G^{\bullet}GG]^{+}$, $[GG^{\bullet}]^{+}$, and $[GGG^{+}]^{+}$. Figure 1 shows the lowest-energy structures for each of the three isomeric α-carbon-centered triglycine radical cations. The N-terminal α-carbon-centered radical ion $[\mathbf{G^{\bullet}GG}]^{+}$**-1** is at the global minimum on the PES: the radical center is attached to powerful π-electron donating (NH_2−) and withdrawing ($[-C(OH)NH]^{+}$) groups; i.e., it is stabilized captodatively.[19,34–36] In addition, $[\mathbf{G^{\bullet}GG}]^{+}$**-1** is stabilized by a seven-membered ring containing a very strong $CO_1{-}H^{+}\cdots O_2C$ hydrogen bond (bond length: 1.436 Å; the italicized subscripts refer to the residue number). $[\mathbf{G^{\bullet}GG}]^{+}$**-1** is 30.3 kcal/mol lower in enthalpy than the lowest energy canonical triglycine radical cation, $H_2N^{\bullet+}CH_2CONHCH_2CONHCH_2COOH$, which has its highest charge and spin on the amino group.

$[\mathbf{GG^{\bullet}G}]^{+}$**-1**, is also a captodative radical ion, stabilized by a relatively weak electron-donating group (−CONH) and a strong electron-withdrawing group ($[-C(OH)NH]^{+}$) attached to the radical center. The delocalization about the α-carbon is smaller than that in $[\mathbf{G^{\bullet}GG}]^{+}$**-1**, as shown by

Table 1. Radical Stabilization Energies (RSEs in kcal/mol) Values of RSE Were Calculated As the Energy Change in the Following Isodesmic Reactions: $R^{\bullet} + CH_4 \rightarrow RH + CH_3^{\bullet}$

$XC^{\bullet}HY + CH_4 \rightarrow XCH_2Y + CH_3^{\bullet}$		
X	Y	RSE
NH_2	H	10.7
H	COOH	5.0
H	$C(OH)_2^{+}$	4.8
NH_2	COOH	22.9
NH_2	$C(OH)_2^{+}$	43.5
CH_3CONH	H	8.9
H	$C(OHNH_2)^{+}$	4.3
CH_3CONH	$C(OH)_2^{+}$	13.3
CH_3CONH	$C(OHNH_2)^{+}$	16.8
NH_2	$C(OHNH_2)^{+}$	19.0

(29) Frisch, M. J. et al. *Gaussian 03*, revision D.01; Gaussian, Inc.: Wallingford, CT, 2004.
(30) Becke, A. D. *J. Chem. Phys.* **1993**, *98*, 5648–5652.
(31) Lee, C. T.; Yang, W. T.; Parr, R. G. *Phys. Rev. B* **1988**, *37*, 785–789.
(32) Gonzales, C.; Schlegel, H. B. *J. Chem. Phys.* **1989**, *90*, 2154–2161.
(33) Boese, A. D.; Martin, J. M. L. *J. Chem. Phys.* **2004**, *121*, 3405–3416.
(34) Sustmann, R.; Korth, H. G. *Adv. Phys. Org. Chem.* **1990**, *26*, 131–178.
(35) Bordwell, F. G.; Zhang, X.; Alnajjar, M. S. *J. Am. Chem. Soc.* **1992**, *114*, 7623–7629.
(36) Easton, C. J. *Chem. Rev.* **1997**, *97*, 53–82.

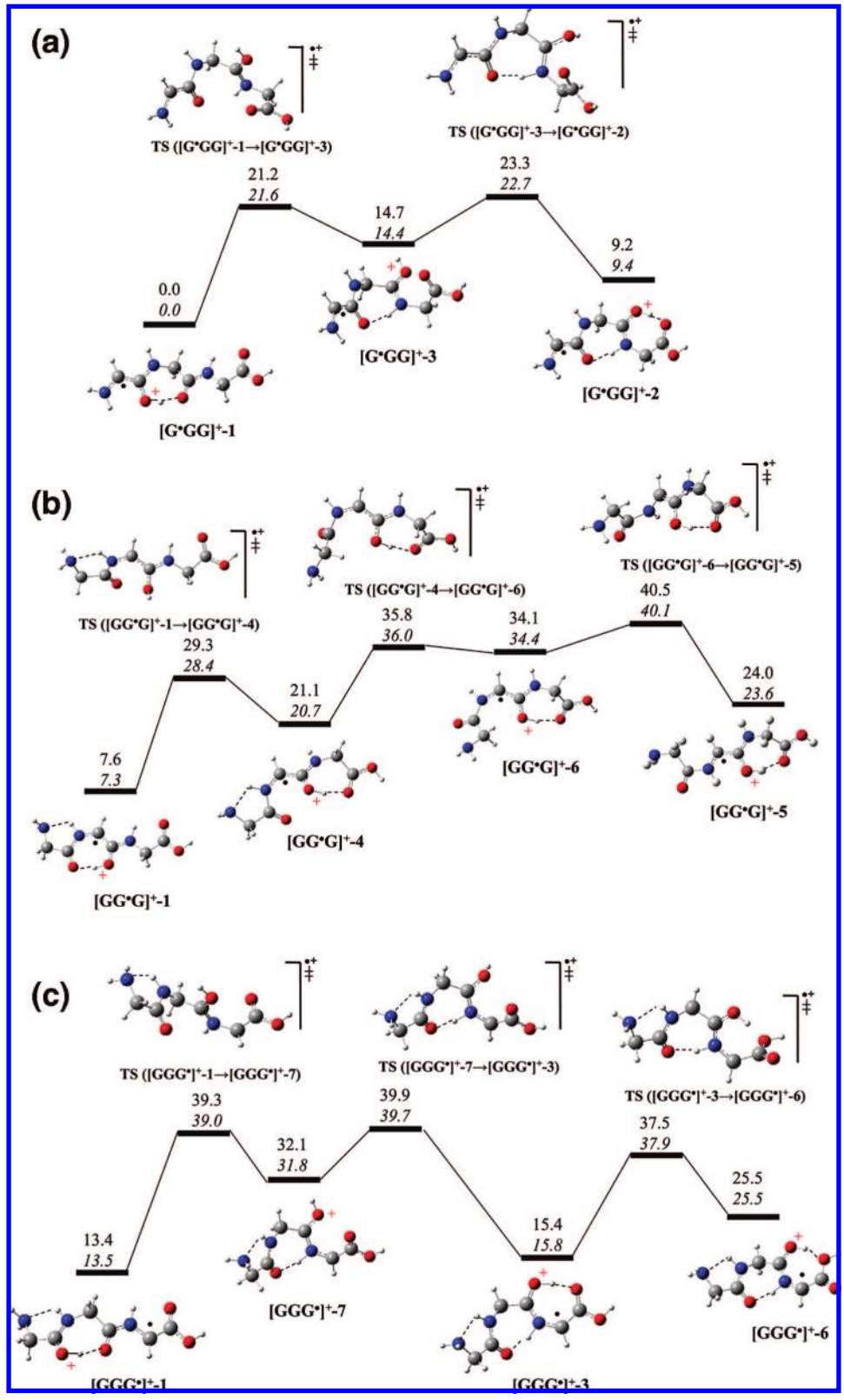

Figure 2. Energy profile for interconversion: (a) between $[\mathbf{G^{\bullet}GG}]^{+}$**-1** and $[\mathbf{G^{\bullet}GG}]^{+}$**-2**; (b) between $[\mathbf{GG^{\bullet}G}]^{+}$**-1** and $[\mathbf{GG^{\bullet}G}]^{+}$**-5**; (c) between $[\mathbf{GGG^{\bullet}}]^{+}$**-1** and $[\mathbf{GGG^{\bullet}}]^{+}$**-6**. Upper numbers are enthalpies at 0 K, and lower italicized numbers are free energies at 298 K. All numbers (in kcal/mol) are relative to $[\mathbf{G^{\bullet}GG}]^{+}$**-1**.

the longer N−C$^{\bullet}$ and C$^{\bullet}$−C bonds; consequently, $[\mathbf{GG^{\bullet}G}]^{+}$**-1** is higher in enthalpy than $[\mathbf{G^{\bullet}GG}]^{+}$**-1** by 7.6 kcal/mol. This finding is consistent with the calculated radical stabilization energy (RSE):[14,19,37] the computed enthalpy for the reaction $XC^{\bullet}HY + CH_4 \rightarrow XCH_2Y + CH_3^{\bullet}$ is 19.0 kcal/mol, when X = NH_2 and Y = $[C(OH)NH_2]^{+}$, and 16.8 kcal/mol, when X = CH_3CONH and Y = $[C(OH)NH_2]^{+}$ (see Table 1), consistent with the better electron-donating properties of the amino relative to the amidic group. $[\mathbf{GG^{\bullet}G}]^{+}$**-1** also contains a seven-membered ring with a short hydrogen bond ($O_1\cdots H^{+}$

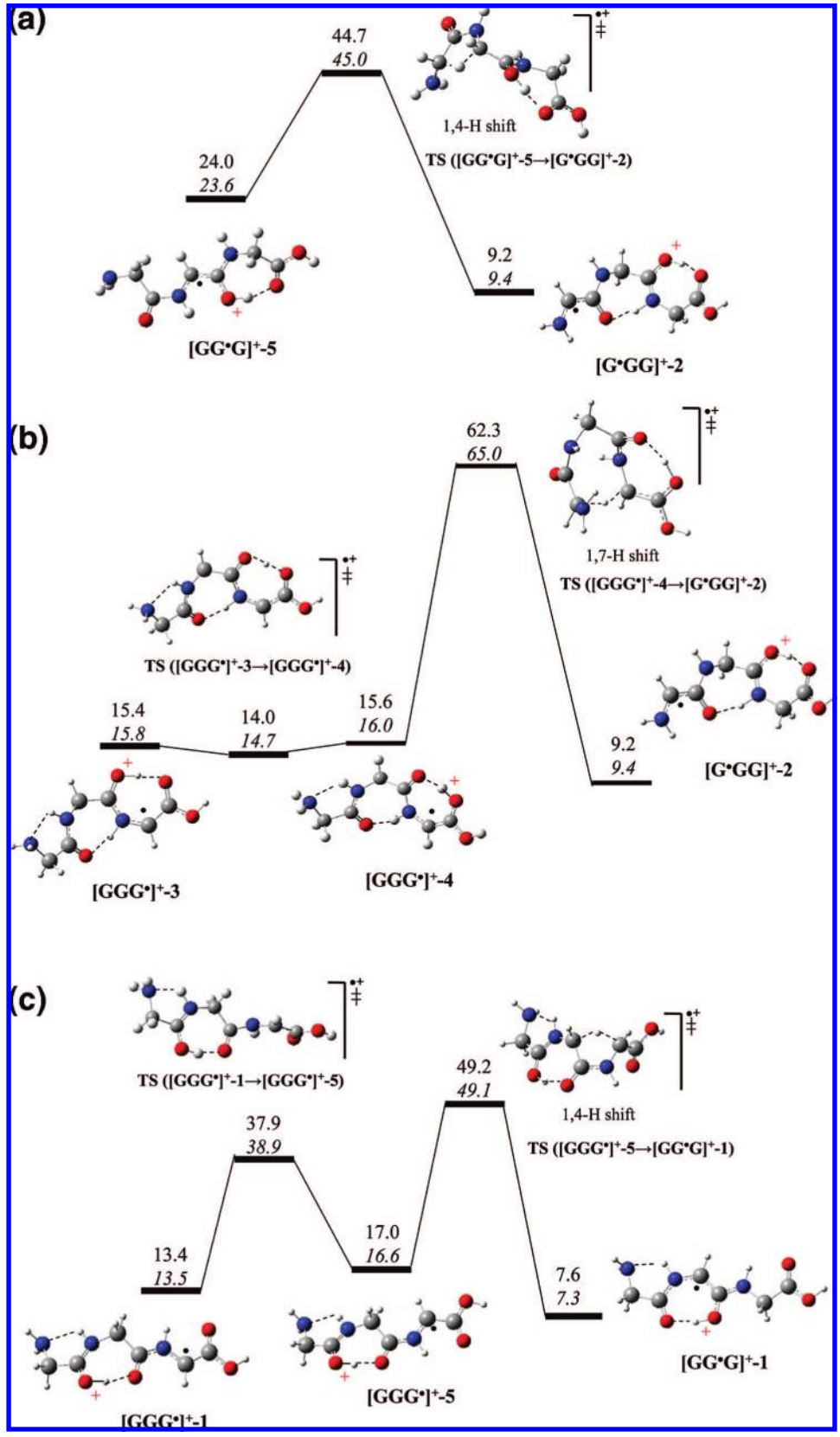

Figure 3. Energy profile for interconversion: (a) between [**GG•G**]$^+$**-5** and [**G•GG**]$^+$**-2**; (b) between [**GGG•**]$^+$**-3** and [**G•GG**]$^+$**-2**; (c) between [**GGG•**]$^+$**-1** and [**GG•G**]$^+$**-1**. Upper numbers are enthalpies at 0 K, and lower italicized numbers are free energies at 298 K. All numbers (in kcal/mol) are relative to [**G•GG**]$^+$**-1**.

length: 1.473 Å) that delocalizes some of the positive charge onto the N-terminal amide group and removes some from the C-terminal amide group, both effects diminishing the captodative stabilization by these substituents. In addition, there is a weak $N_3H\cdots O_3$ hydrogen bond (2.113 Å) that delocalizes some positive charge onto the carboxyl group.

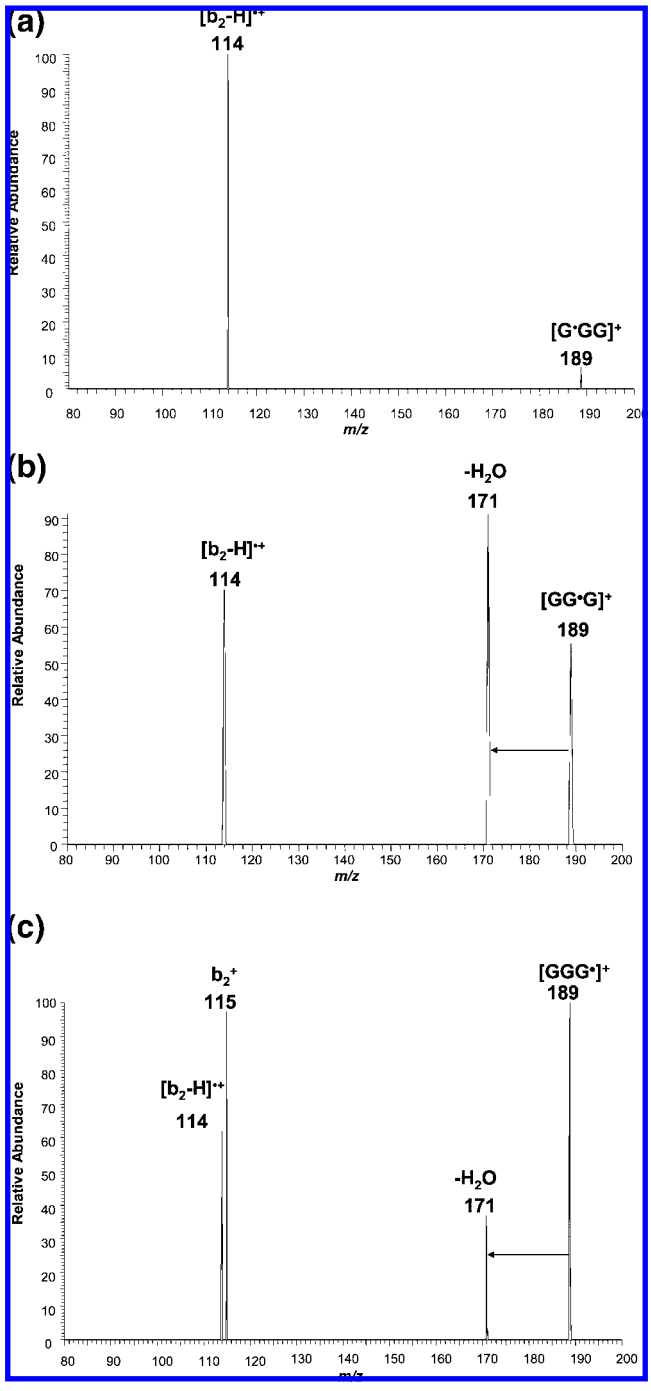

Figure 4. CID mass spectra (at the MS^4 stage) of (a) $[G^{\bullet}GG]^+$ formed from $[Y^{\bullet}GG]^+$ (relative collision energy: 20% with L = 4Cl-tpy); (b) $[GG^{\bullet}G]^+$ formed from $[GY^{\bullet}G]^+$ (relative collision energy: 20% with L = 12-crown-4); (c) $[GGG^{\bullet}]^+$ formed from $[GGY^{\bullet}]^+$ (relative collision energy: 20% with L = 12-crown-4).

$[\mathbf{GGG^{\bullet}}]^+$**-1** is higher in enthalpy than the structure at the global minimum, $[\mathbf{G^{\bullet}GG}]^+$**-1**, by 13.4 kcal/mol. In $[\mathbf{GGG^{\bullet}}]^+$**-1**, the proton detached from the α-carbon of the third residue is located on the oxygen atom of the N-terminal peptide bond and is hydrogen-bonded to the carbonyl oxygen atom of the C-terminal peptide bond (the CO_1-$H^+\cdots O_2C$ hydrogen bond length: 1.452 Å). Unlike in the other two isomers, the charge and spin in $[\mathbf{GGG^{\bullet}}]^+$**-1** are essentially located in separate regions. The C-terminal amide bond (1.353 Å) in $[\mathbf{GGG^{\bullet}}]^+$**-1** is longer than that in the other two isomers, indicating that the positive charge is less effectively delocalized onto the C-terminal residue; hence the charge is predominantly on the N-terminal residue, and the spin, on the C-terminal residue.

Figure 2 shows other low-energy structures of the $[G^{\bullet}GG]^+$, $[GG^{\bullet}G]^+$, and $[GGG^{\bullet}]^+$ radical cations and the barriers against interconversion to their respective lowest energy isomers, $[\mathbf{G^{\bullet}GG}]^+$**-1**, $[\mathbf{GG^{\bullet}G}]^+$**-1**, and $[\mathbf{GGG^{\bullet}}]^+$**-1**. More than 30 structures per each of the three triglycine radical cations were examined; in addition, more than 15 canonical structures were considered, resulting in a study involving >105 triglycine radical cation structures. The low-energy structures presented in Figure 2 were selected because they are key intermediates involved in interconversions among $[G^{\bullet}GG]^+$, $[GG^{\bullet}G]^+$, and $[GGG^{\bullet}]^+$; this set of structures is not intended to be exhaustive, as there are many low-energy structures on the potential energy surfaces. The tautomerism of three $[G^{\bullet}GG]^+$ isomers is shown in Figure 2a: For $[\mathbf{G^{\bullet}GG}]^+$**-1**, rotations about the C_α−C bond of the second residue and the N−C_α bond of the third residue plus proton transfer from the carbonyl oxygen of the first residue to the carbonyl oxygen of the second residue give $[\mathbf{G^{\bullet}GG}]^+$**-3**, which is 14.7 kcal/mol higher in enthalpy than $[\mathbf{G^{\bullet}GG}]^+$**-1**. The barrier against this tautomeric reaction is 21.2 kcal/mol. Rotation about the C═O_2H^+ bond results in formation of a hydrogen bond between the proton and the C-terminal carbonyl oxygen in $[\mathbf{G^{\bullet}GG}]^+$**-2**, which is above $[\mathbf{G^{\bullet}GG}]^+$**-1** by only 9.2 kcal/mol; the barrier against this isomerization step is 23.3 kcal/mol, relative to $[\mathbf{G^{\bullet}GG}]^+$**-1**.

Figure 2b shows the interconversion of four $[GG^{\bullet}G]^+$ isomers, of which $[\mathbf{GG^{\bullet}G}]^+$**-1**, the starting isomer, has its peptide bonds in a *trans*/*trans* configuration, while $[\mathbf{GG^{\bullet}G}]^+$**-5**, the product isomer, has a *cis*/*trans* configuration. For $[\mathbf{GG^{\bullet}G}]^+$**-1**, rotating about the N−C_α bond of the third residue, breaking the $CO_1\cdots H^+$−O_2C hydrogen bond and forming the CO_2−$H^+\cdots O_3C$ hydrogen bond between the proton and the C-terminal carbonyl oxygen result in $[\mathbf{GG^{\bullet}G}]^+$**-4**, which is 13.5 kcal/mol in enthalpy above $[\mathbf{GG^{\bullet}G}]^+$**-1**, or 21.1 kcal/mol above $[\mathbf{G^{\bullet}GG}]^+$**-1**, the structure at the global minimum. A contribution to this difference is that the hydrogen bond in $[\mathbf{GG^{\bullet}G}]^+$**-4** is weaker, as the carbonyl oxygen of the carboxylic acid is less basic than that of the amide. The barrier against this isomerization step from $[\mathbf{GG^{\bullet}G}]^+$**-1** to $[\mathbf{GG^{\bullet}G}]^+$**-4** is 29.3 kcal/mol above $[\mathbf{G^{\bullet}GG}]^+$**-1**. Rotation about the first peptide bond in $[\mathbf{GG^{\bullet}G}]^+$**-4** from *trans* to *cis* results in $[\mathbf{GG^{\bullet}G}]^+$**-6**, which is 13.0 kcal/mol higher in enthalpy than $[\mathbf{GG^{\bullet}G}]^+$**-4**. The barrier against this *trans*-to-*cis* isomerization step is 14.7 kcal/mol. Rotation about the N−C_α bond of the second residue in $[\mathbf{GG^{\bullet}G}]^+$**-6** from *cis* to *trans* (with respect to the two hydrogens) gives a lower-energy isomer $[\mathbf{GG^{\bullet}G}]^+$**-5**, which is only 24.0 kcal/mol above $[\mathbf{G^{\bullet}GG}]^+$**-1**. This isomerization step from $[\mathbf{GG^{\bullet}G}]^+$**-6** to $[\mathbf{GG^{\bullet}G}]^+$**-5** has the highest cumulative barrier, 40.5 kcal/mol, in Figure 2b. We will see later that $[\mathbf{GG^{\bullet}G}]^+$**-5** has the crucial configuration that permits a 1,4-hydrogen atom transfer from the α-carbon of the first residue to the α-carbon of the second residue, which in consequence effects "transfer" of the radical center in the opposite direction.

Figure 2c shows the interconversion of four critical $[GGG^{\bullet}]^+$ isomers. Transfer of the proton from the oxygen of the first to that of the second residue plus rotation about the C_α−C bond of the second residue in $[\mathbf{GGG^{\bullet}}]^+$**-1** results in $[\mathbf{GGG^{\bullet}}]^+$**-7**, which is 32.1 kcal/mol above $[\mathbf{G^{\bullet}GG}]^+$**-1**. Rotation about the C═O_2H^+ bond and hydrogen-bonding with carbonyl oxygen of the carboxylic group then gives $[\mathbf{GGG^{\bullet}}]^+$**-3**. This is a rather low-lying isomer—only 2.0 kcal/mol above $[\mathbf{GGG^{\bullet}}]^+$**-1**, or 15.4 kcal/mol above $[\mathbf{G^{\bullet}GG}]^+$**-1**, the structure at the global minimum.

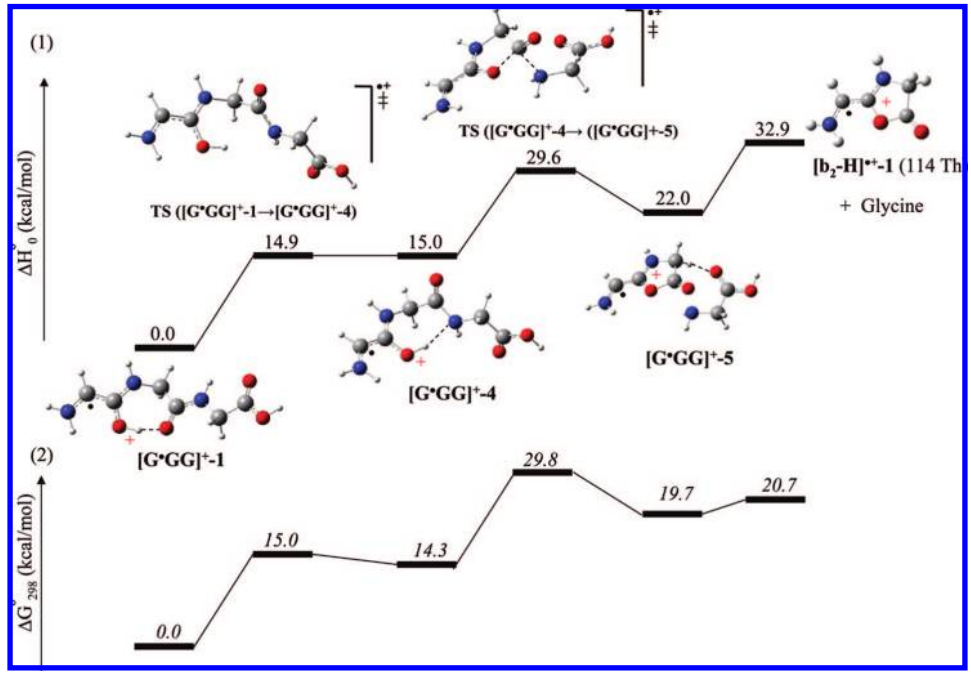

Figure 5. Energy profiles for the loss of glycine from $[G^{\bullet}GG]^{+}$: The upper profile with normal font shows enthalpies at 0 K. The lower profile with italicized font shows free energies at 298 K; refer to the upper profile for structures.

Rotation about the C_{α}−C bond of the third residue in $[\mathbf{GGG^{\bullet}}]^{+}$**-3** gives $[\mathbf{GGG^{\bullet}}]^{+}$**-6**, the tautomer that has the critical configuration permitting a subsequent elimination of water (*vide infra*). The barriers to the isomerization steps are fairly similar; the largest barrier, at 39.9 kcal/mol, is the one between $[\mathbf{GGG^{\bullet}}]^{+}$**-7** and $[\mathbf{GGG^{\bullet}}]^{+}$**-3**.

3.2. Interconversions among $[G^{\bullet}GG]^{+}$, $[GG^{\bullet}G]^{+}$, and $[GGG^{\bullet}]^{+}$. We consider in this section the barriers against interconversions among $[G^{\bullet}GG]^{+}$, $[GG^{\bullet}G]^{+}$, and $[GGG^{\bullet}]^{+}$, i.e., the mobility of the radical site. This is analogous to an analysis on the mobility of the ionizing proton among tautomers of protonated triglycine.[27] Our strategy in studying the interconversions among the triglycine radical cations was to determine the lowest-energy transition structures (TSs) for H-atom transfer and then, using IRC analyses, follow the reaction paths downhill on both sides of the TS to determine which conformers of the reactants and products were involved.

3.2.1. Conversion from $[GG^{\bullet}G]^{+}$ to $[G^{\bullet}GG]^{+}$. Figure 3a shows the energy profile for the tautomerism reaction from $[\mathbf{GG^{\bullet}G^{+}}]$**-5** to $[\mathbf{G^{\bullet}GG}]^{+}$**-2** via a 1,4-H atom transfer from the α-carbon of the first residue to that of the second residue. The barrier against this radical-transfer step is relatively high, 44.7 kcal/mol relative to $[\mathbf{G^{\bullet}GG}]^{+}$**-1** and 37.1 kcal/mol relative to $[\mathbf{GG^{\bullet}G^{+}}]$**-1**. By contrast, proton transfers in protonated triglycine are much lower in energy, <17 kcal/mol, relative to the global minimum structure.[27] The forward barrier from $[\mathbf{GG^{\bullet}G^{+}}]$**-5** is 20.7 kcal/mol, comparable to the barrier (23.6 kcal/mol) reported by Moran et al.[38] in their 1,4-H atom transfer in the reaction $H_2C^{\bullet}CONHCH_3 = H_3CCONHC^{\bullet}H_2$; the reverse barrier is 35.5 kcal/mol, higher but not too significantly than the barrier of 29.7 kcal/mol reported by Moran et al.[38] A contributing factor to the differences is that we are dealing with the radical *cation* of a tripeptide, while they examined a *neutral* model of the peptide bond.

3.2.2. Conversion from $[GGG^{\bullet}]^{+}$ to $[G^{\bullet}GG]^{+}$. Figure 3b shows the energy profile for the tautomerism reactions from $[\mathbf{GGG^{\bullet}}]^{+}$**-3**, to $[\mathbf{GGG^{\bullet}}]^{+}$**-4**, and then to $[\mathbf{G^{\bullet}GG}]^{+}$**-2**, the latter step, a 1,7-H atom transfer between the α-carbons of the first and the third residues, transfers the radical in the opposite direction. The barrier against converting $[GGG^{\bullet}]^{+}$ to $[G^{\bullet}GG]^{+}$, at 62.3 kcal/mol relative to $[\mathbf{G^{\bullet}GG}]^{+}$**-1**, is considerably higher than that against converting $[GG^{\bullet}G]^{+}$ to $[G^{\bullet}GG]^{+}$ (at 44.7 kcal/mol, *vide supra*). The forward barrier from $[\mathbf{GGG^{\bullet}}]^{+}$**-4** is 46.7 kcal/mol, whereas the reverse barrier from $[\mathbf{G^{\bullet}GG}]^{+}$**-2** is 53.1 kcal/mol, both considerably larger than the barriers of 23.9 and 18.4 kcal/mol, respectively, against the 1,7-atom transfer reported by Moran et al.[38] The major difference is that interconversion between $[\mathbf{GGG^{\bullet}}]^{+}$**-4** and $[\mathbf{G^{\bullet}GG}]^{+}$**-2** involves cleavage and formation of hydrogen bonds that are absent in the *neutral* model.

3.2.3. Conversion from $[GGG^{\bullet}]^{+}$ to $[GG^{\bullet}G]^{+}$. This energy profile is shown in Figure 3c. Rotation about the second peptide bond in $[\mathbf{GGG^{\bullet}}]^{+}$**-1** from *trans* to *cis* gives $[\mathbf{GGG^{\bullet}}]^{+}$**-5**, which is 17.0 kcal/mol above $[\mathbf{G^{\bullet}GG}]^{+}$**-1**. This isomerization step has a relatively high barrier of 37.9 kcal/mol above $[\mathbf{G^{\bullet}GG}]^{+}$**-1**. $[\mathbf{GGG^{\bullet}}]^{+}$**-5** has the appropriate configuration for a 1,4-H atom transfer from the α-carbon of the second residue to that of the third residue to give $[\mathbf{GG^{\bullet}G}]^{+}$**-1**. The barrier against this radical-transfer step is 49.2 kcal/mol relative to $[\mathbf{G^{\bullet}GG}]^{+}$**-1**. In short, all three radical-transfer reactions have relatively high barriers (≥44.7 kcal/mol), which means that there is a good probability that the $[G^{\bullet}GG]^{+}$, $[GG^{\bullet}G]^{+}$, and $[GGG^{\bullet}]^{+}$ ions produced by CID of $[Y^{\bullet}GG]^{+}$, $[GY^{\bullet}G]^{+}$, and $[GGY^{\bullet}]^{+}$ are stable and isomerically pure. These barriers are all considerably higher than the intramolecular proton-transfer barriers of <17 kcal/mol encountered in protonated triglycine.[27]

3.3. Low-Energy Experiments of $[G^{\bullet}GG]^{+}$, $[GG^{\bullet}G]^{+}$, and $[GGG^{\bullet}]^{+}$. The radical cations $[Y^{\bullet}GG]^{+}$, $[GY^{\bullet}G]^{+}$, and $[GGY^{\bullet}]^{+}$ were first produced via CID of the complexes $[Cu^{II}(L)(M)]^{\bullet 2+}$ (M = YGG, GYG, and GGY, respectively). Subsequent fragmentations of the radical ions resulted in the loss of the tyrosine side chain as *p*-quinomethide to produce the three isomeric triglycine radical cations: $[G^{\bullet}GG]^{+}$, $[GG^{\bullet}G]^{+}$, and $[GGG^{\bullet}]^{+}$, respectively. Subjecting these three

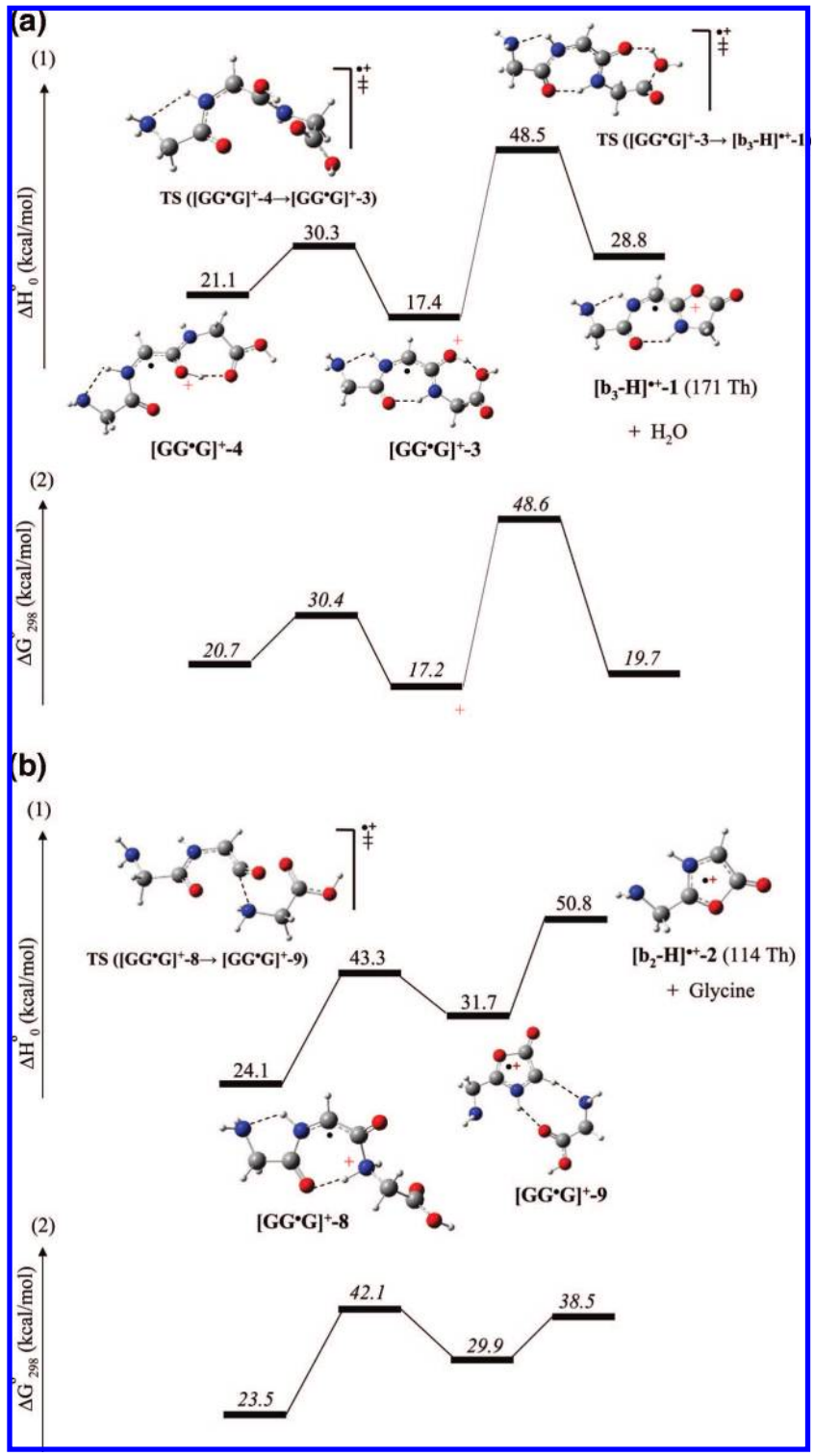

Figure 6. Energy profiles for the loss of (a) H_2O from $[GG^{\bullet}G]^+$ and (b) glycine from $[GG^{\bullet}G]^+$. The upper profile with normal font shows enthalpies at 0 K. The lower profile with italicized font shows free energies at 298 K; refer to the upper profile for structures. All numbers (in kcal/mol) are relative to $[\mathbf{G^{\bullet}GG}]^+$**-1**.

radical cations to collisional activation resulted in different product ions or different distributions of product ions; these findings substantiate the thesis that the three precursor ions have different initial structures. Figure 4a shows a typical product ion spectrum of $[G^{\bullet}GG]^+$; the lone fragment ion at 114 Th is the $[b_2 - H]^{\bullet+}$ ion. Increasing the collision energy leads to a second product ion at 86 Th, the $[a_2 - H]^{\bullet+}$ ion (not shown). These ions have previously been reported in a study of the $[G^{\bullet}GG]^+$ ion generated via CID of $[WGG]^{\bullet+}$.[7] Confirmation of the fragmentation products has been established here via the CID of $[G^{\bullet}AG]^+$ and $[G^{\bullet}GA]^+$. In the former, the $[b_2 - H]^{\bullet+}$ ion at 128 Th was observed, thus implying the elimination of a neutral glycine; in the latter, the $[b_2 - H]^{\bullet+}$ ion at 114 Th was observed, verifying the elimination of the C-terminal residue, a neutral alanine in this case.

A typical product ion spectrum of the $[GG^{\bullet}G]^+$ ion (Figure 4b) also shows a prominent product ion at 114 Th; in addition, there is an equally abundant product ion at 171 Th, formed via elimination of H_2O to give the $[b_3 - H]^{\bullet+}$ ion. It should be noted that the 171 Th ion was not observed in the CID of $[G^{\bullet}GG]^+$ under all collision energies investigated (from low energies that gave no product ions to high energies that showed almost complete fragmentation of $[G^{\bullet}GG]^+$). Dissociation of the $[GGG^{\bullet}]^+$ ion (Figure 4c) also gives the ions at 114 and 171 Th, but there is a third abundant product, assigned as the b_2^+ ion, at 115 Th. This last ion was not observed in the CID spectra of $[G^{\bullet}GG]^+$ and $[GG^{\bullet}G]^+$. Thus the product ion spectra of the three triglycine radical cations—$[G^{\bullet}GG]^+$, $[GG^{\bullet}G]^+$, and $[GGG^{\bullet}]^+$—are all substantially different and support the above DFT results that the three radical cations have distinct initial structures. Of all the product ions discussed, only the b_2^+ ion is observed in the CID of protonated GGG under typical conditions.[39]

3.4. Potential-energy Surfaces for the Fragmentations of $[G^{\bullet}GG]^+$, $[GG^{\bullet}G]^+$, and $[GGG^{\bullet}]^+$. 3.4.1. $[G^{\bullet}GG]^+$. Figure 5 shows the PES leading to the formation of the $[b_2 - H]^{\bullet+}$ ion and neutral glycine. The dissociation of $[\mathbf{G^{\bullet}GG}]^+$**-1** proceeds through a critical intermediate $[\mathbf{G^{\bullet}GG}]^+$**-4**: rotation about the C_α—C bond of the second glycine residue and replacement of the CO_1—$H^+\cdots O_2C$ hydrogen bond in $[\mathbf{G^{\bullet}GG}]^+$**-1** by a weaker CO_1—$H^+\cdots$NH hydrogen bond result in $[\mathbf{G^{\bullet}GG}]^+$**-4**, which is 15.0 kcal/mol higher in enthalpy. Transfer of the proton to the amide nitrogen of the C-terminal peptide bond, followed by nucleophilic attack by the carbonyl oxygen of the N-terminal peptide bond on the carbonyl carbon of the C-terminal peptide bond with concomitant elimination of the C-terminal residue, results in a complex that has the $[b_2 - H]^{\bullet+}$ ion solvated by a neutral glycine. Dissociation of this complex produces $[\mathbf{b_2} - \mathbf{H}]^{\bullet+}$**-1** and glycine. These products have the highest energy, 32.9 kcal/mol above $[\mathbf{G^{\bullet}GG}]^+$**-1**. Relative to the barrier of 44.7 kcal/mol against converting $[\mathbf{G^{\bullet}GG}]^+$**-2** into $[\mathbf{GG^{\bullet}G}]^+$**-4** (Figure 3a), this barrier against dissociation of $[\mathbf{G^{\bullet}GG}]^+$**-1** to give $[\mathbf{b_2} - \mathbf{H}]^{\bullet+}$**-1** and glycine is much lower and is consistent with the experimental results shown in Figure 4, suggesting that dissociation is energetically more favorable than isomerization. The $[\mathbf{b_2} - \mathbf{H}]^{\bullet+}$**-1** ion is an oxazolone that is stabilized by a strong captodative interaction: it has a C_α radical site bracketed by a good electron donor (the amino group) and a powerful electron acceptor (the positively charged oxazolone ring).

3.4.2. $[GG^{\bullet}G]^+$. The PES leading to the loss of H_2O from $[\mathbf{GG^{\bullet}G}]^+$**-1** is given in Figure 6a. $[\mathbf{GG^{\bullet}G}]^+$**-1** first converts to $[\mathbf{GG^{\bullet}G}]^+$**-4**, as shown in Figure 2b. Rotations about the C_α—C bonds of the second and third residues then ensue to produce $[\mathbf{GG^{\bullet}G}]^+$**-3**. The barrier against the isomerization step from $[\mathbf{GG^{\bullet}G}]^+$**-4** is only 9.2 kcal/mol (30.3 relative to $[\mathbf{G^{\bullet}GG}]^+$**-1**). $[\mathbf{GG^{\bullet}G}]^+$**-3** has the critical configuration that facilitates the loss of water: proton migration from the carbonyl oxygen of the second peptide bond to the hydroxyl oxygen of the carboxylic group, and concomitant nucleophilic attack by the carbonyl oxygen on the carboxyl carbon and cleavage of the C—OH_2^+ bond result in the $[\mathbf{b_3} - \mathbf{H}]^{\bullet+}$**-1** ion and water. The cumulative barrier for this last step is relatively high at 48.5 kcal/mol versus $[\mathbf{G^{\bullet}GG}]^+$**-1**. The $[\mathbf{b_3} - \mathbf{H}]^{\bullet+}$**-1** ion, like the $[\mathbf{b_2} - \mathbf{H}]^{\bullet+}$**-1** ion, is also an oxazolone stabilized by a captodative structure; here, however, the electron donor, NH_2CH_2CONH—, is much weaker. $[\mathbf{GG^{\bullet}G}]^+$**-3** is structurally very similar to $[\mathbf{GG^{\bullet}G}]^+$**-2**, which is formed from the former by a 180° rotation about the C_α—C bond in the third residue. The hydrogen bond between the CO_2—$H^+\cdots O_3C$ in $[\mathbf{GG^{\bullet}G}]^+$**-2** (see Supporting Information) is stronger than that between the CO_2—$H^+\cdots(O_3H)C$ in $[\mathbf{GG^{\bullet}G}]^+$**-3**, resulting in $[\mathbf{GG^{\bullet}G}]^+$**-2** being only 11.7 kcal/mol above $[\mathbf{G^{\bullet}GG}]^+$**-1** in enthalpy.

Formation of the 114 Th ion and the loss of neutral glycine from $[GG^{\bullet}G]^+$ can have two possible routes: $[GG^{\bullet}G]^+$ can tautomerize first to $[G^{\bullet}GG]^+$, which then fragments to give the $[b_2 - H]^{\bullet+}$ ion and glycine. As noted earlier, the rate-determining step against this multistep process is 44.7 kcal/mol (the conversion of $[\mathbf{GG^{\bullet}G}]^+$**-3** to $[\mathbf{G^{\bullet}GG}]^+$**-2** in Figure 3a); all other steps have lower barriers (Figures 2a,b and 5). Alternatively, $[GG^{\bullet}G]^+$ can fragment directly via $[\mathbf{GG^{\bullet}G}]^+$**-8** (Figure 6b), which is protonated on the C-terminal amide nitrogen. As before, nucleophilic attack by the carbonyl oxygen of the N-terminal peptide bond on the carbonyl carbon of the C-terminal peptide bond, with concomitant cleavage of the C-terminal glycine, results in an oxazolone radical cation solvated by glycine; this complex dissociates to give the $[\mathbf{b_2} - \mathbf{H}]^{\bullet+}$**-2** ion. The $[\mathbf{b_2} - \mathbf{H}]^{\bullet+}$**-2** ion is 17.9 kcal/mol higher in enthalpy than its isomeric $[\mathbf{b_2} - \mathbf{H}]^{\bullet+}$**-1** ion; this difference in energy is attributed to the lack of captodative stabilization in $[\mathbf{b_2} - \mathbf{H}]^{\bullet+}$**-2**, which has both its spin and charge residing on the oxazolone ring. The combination of $[\mathbf{b_2} - \mathbf{H}]^{\bullet+}$**-2** and glycine has the highest energy on the PES at 50.8 kcal/mol versus $[\mathbf{G^{\bullet}GG}]^+$**-1**. This direct dissociation of $[GG^{\bullet}G]^+$ involves fewer steps than the indirect dissociation after tautomerism first to $[G^{\bullet}GG]^+$ and may compete efficiently in a mass spectrometry experiment in which the observation window is in the order of tens of microseconds. The dissociation of $[GG^{\bullet}G]^+$ to give the $[b_3 - H]^{\bullet+}$ ion and water has a barrier that is quite comparable to those of the two dissociation routes that result in the $[b_2 - H]^{\bullet+}$ ion and glycine. Thus, the DFT results are consistent with the mass spectrometric observations of both the 114 and 171 Th product ions. The critical barriers are summarized in Table 2.

Table 2. Critical Barriers against Dissociations (ΔH°_0, kcal/mol)[a]

	$[b_2 - H]^{\bullet+}$		$[b_3 - H]^{\bullet+}$		
precursor	direct	indirect	direct	indirect	b_2^+
$[G^{\bullet}GG]^+$	32.9	---	---	---	---
$[GG^{\bullet}G]^+$	50.8	44.7	48.5	---	---
$[GGG^{\bullet}]^+$	---	49.2	45.9	49.2	49.3

[a] Determined by UB3LYP/6−31++G(d,p), all referenced to $[\mathbf{G^{\bullet}GG}]^+$**-1**, the global minimum structure.

3.4.3. $[GGG^{\bullet}]^+$. The elimination of H_2O to give the $[b_3 - H]^{\bullet+}$ ion can conceptually proceed via two possible routes: $[GGG^{\bullet}]^+$ can first tautomerize to $[GG^{\bullet}G]^+$, which then dissociates, or it can dissociate directly to yield the products. The barrier against the tautomerism of $[\mathbf{GGG^{\bullet}}]^+$**-1** to $[\mathbf{GG^{\bullet}G}]^+$**-1** is 49.2 kcal/mol (Figure 3c), which is comparable to the barrier of 48.5 kcal/mol against the dissociation of $[\mathbf{GG^{\bullet}G}]^+$**-1** to $[\mathbf{b_3} - \mathbf{H}]^{\bullet+}$**-1** and glycine (Figure 6a). Figure 7a shows the PES for the direct dissociation of $[GGG^{\bullet}]^+$; tautomer $[\mathbf{GGG^{\bullet}}]^+$**-6** (Figure 2c), discussed previously, has the critical configuration that permits the loss of water. Transfer of the proton from the carbonyl oxygen of the second peptide bond to the hydroxyl oxygen of the carboxylic group, followed by nucleophilic attack by the carbonyl oxygen on

(37) Croft, A. K.; Easton, C. J.; Radom, L. *J. Am. Chem. Soc.* **2003**, *125*, 4119–4124.
(38) Moran, D.; Jacob, R.; Wood, G. P. E.; Coote, M. L.; Davies, M. J.; O'Hair, R. A. J.; Easton, C. J.; Radom, L. *Helv. Chim. Acta* **2006**, *89*, 2254–2272.
(39) El Aribi, H.; Rodriquez, C. F.; Almeida, D. R. P.; Ling, Y.; Mak, W. W.-N.; Hopkinson, A. C.; Siu, K. W. M. *J. Am. Chem. Soc.* **2003**, *125*, 9229–9236.

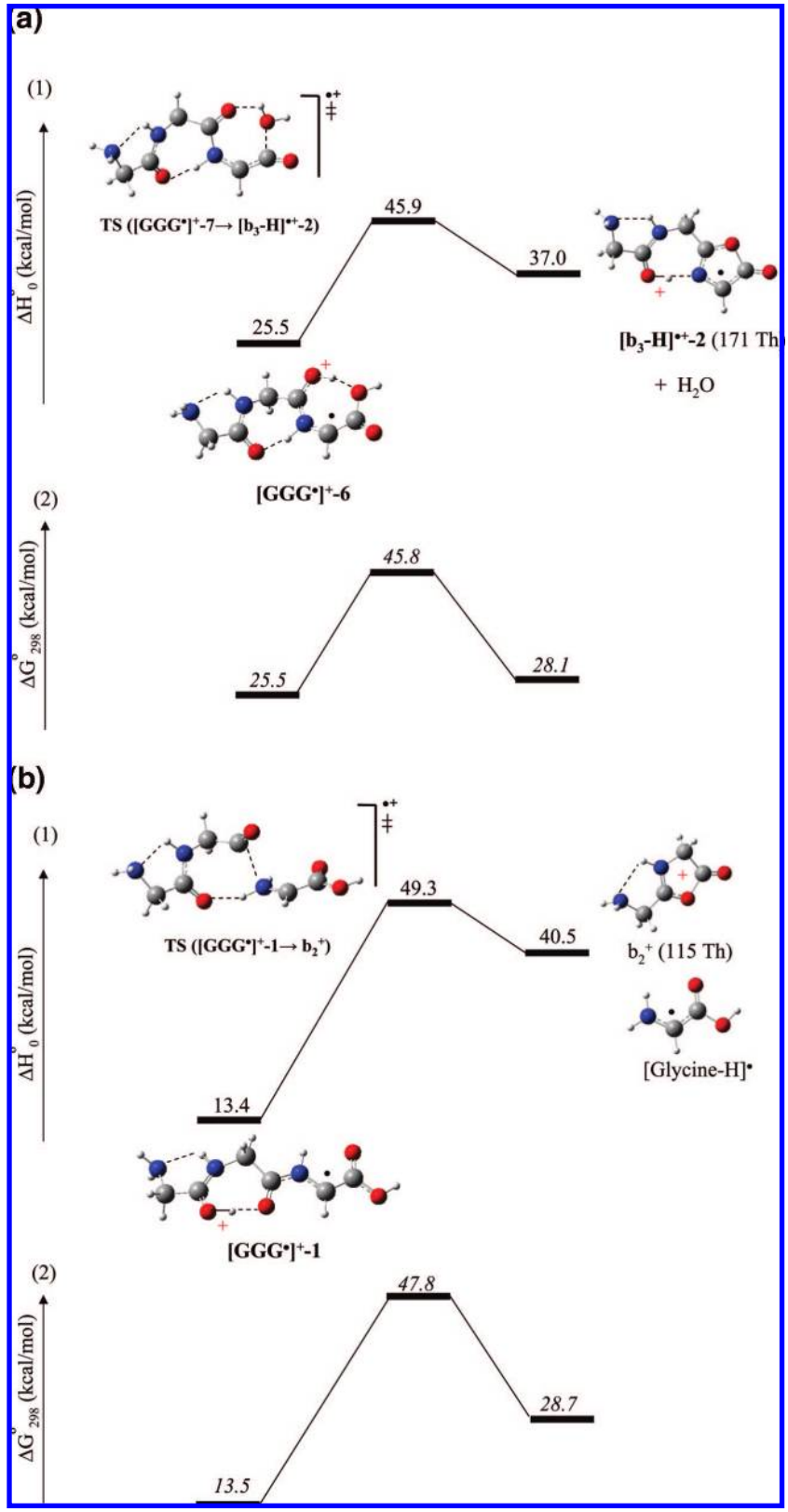

Figure 7. Energy profiles for (a) the loss of H_2O from $[GGG^{\bullet}]^+$ and (b) the formation of the b_2^+ ion from $[GGG^{\bullet}]^+$. The upper profile with normal font shows enthalpies at 0 K. The lower profile with italicized font shows free energies at 298 K; refer to the upper profile for structures. All numbers (in kcal/mol) are relative to $[\mathbf{G^{\bullet}GG}]^+$**-1**.

the carbon of the carboxylic group with concomitant extension of the $C_3-OH_2^+$ bond, results in the $[\mathbf{b_3 - H}]^{\bullet+}$**-2** ion and neutral water. These products are 37.0 kcal/mol while the barrier is 45.9 kcal/mol above $[\mathbf{G^{\bullet}GG}]^+$**-1**. Thus the indirect and direct channels have barriers that differ only by ~3 kcal/mol.

Formation of the $[b_2 - H]^{\bullet+}$ ion and glycine from $[GGG^{\bullet}]^+$ necessarily involves migration of the radical site. The lowest

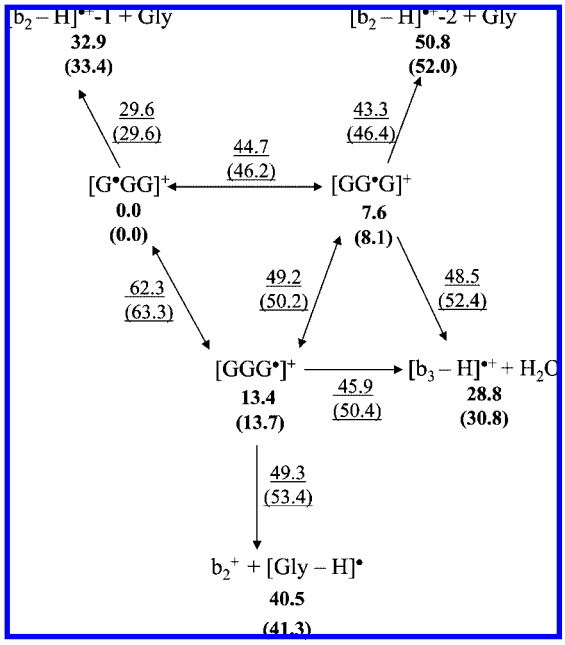

Figure 8. Interconversions and dissociations of triglycine radical cations. Bolded numbers are enthalpies at 0 K; underscored numbers are the reaction barriers, all relative to the structure at global minimum, $[\mathbf{G^{\bullet}GG}]^{+}$**-1**. The upper numbers were determined at the UB3LYP/6−31++G(d,p), and the lower numbers in parentheses, at the UBMK/6−31++G(d,p) level of theory.

energy pathway is one in which $[\mathbf{GGG^{\bullet}}]^{+}$**-1** tautomerizes first to $[\mathbf{GG^{\bullet}G}]^{+}$**-1**, which as previously discussed has a barrier of 49.2 kcal/mol versus $[\mathbf{G^{\bullet}GG}]^{+}$**-1** (Figure 3c). $[\mathbf{GG^{\bullet}G}]^{+}$**-1** then dissociates to give $[\mathbf{b_2 - H}]^{\bullet+}$**-1** and glycine (Figure 5 shows the indirect route via $[\mathbf{G^{\bullet}GG}]^{+}$**-1**, *vide supra*). Thus the barriers against dissociation of $[GGG^{\bullet}]^{+}$ to the $[b_3 - H]^{\bullet+}$ and the $[b_2 - H]^{\bullet+}$ ions are comparable.

The product ion spectrum of the $[GGG^{\bullet}]^{+}$ ion in Figure 4c shows the presence of a third product, the b_2^{+} ion. Figure 7b shows the PES for the dissociation of $[\mathbf{GGG^{\bullet}}]^{+}$**-1** to the b_2^{+} ion and the glycyl radical. Again, the dissociation proceeds by first proton transfer to the amide nitrogen of the second peptide bond, followed by cyclization to form the oxazolone ring with concomitant extension of the $OC-NH_2^{+}$ bond that results in elimination of the glycyl radical. The barrier against this reaction is 49.3 kcal/mol relative to $[\mathbf{G^{\bullet}GG}]^{+}$**-1**, which is comparable to the barriers against dissociations into the $[b_3 - H]^{\bullet+}$ and the $[b_2 - H]^{\bullet+}$ ions (Table 2). These DFT results tell us that all three dissociation channels are competitive, as observed experimentally (Figure 4c).

Thus, we have shown by DFT calculations and tandem mass spectrometry that the radical sites in the three triglycine radical cations—$[G^{\bullet}GG]^{+}$, $[GG^{\bullet}G]^{+}$, and $[GGG^{\bullet}]^{+}$—are relatively immobile. Interconversions between the isomeric radical cations have barriers ≥44.7 kcal/mol relative to the structure at the global minimum; these are much larger than the barriers against interconversions between tautomers of protonated triglycine at <17 kcal/mol (again relative to the global minimum structure).[27] Experimentally, the three triglycine radical cations were formed via collision-induced dissociations of copper(II)-containing tertiary complex ions that contain YGG, GYG, and GGY. The $[G^{\bullet}GG]^{+}$, $[GG^{\bullet}G]^{+}$, and $[GGG^{\bullet}]^{+}$ ions thus formed, when subjected to collisional activation, give different product ion spectra with increasing complexity from $[G^{\bullet}GG]^{+}$ to $[GG^{\bullet}G]^{+}$ and to $[GGG^{\bullet}]^{+}$, thereby corroborating the thesis that these ions have distinct initial radical sites and structures. Formation of some of the product ions is likely preceded by interconversion between the triglycine radical cations as direct and indirect dissociations (the latter after interconversion) have comparable barriers.

Figure 8 summarizes the relative enthalpies of the isomeric triglycine radical cations and their dissociation products (bolded) and the reaction barriers (underscored). The values in brackets are those obtained by UBMK after full geometric optimization starting with the UB3LYP structures. The BMK functional has been found to have an accuracy in the 2 kcal/mol range for transition structures,[33] which does not come at the expense of equilibrium properties; the accuracies of BMK for H-atom transfers were recently verified in a comparison against high-level composite methods, including G3(MP2)-RAD and CBS-QB3.[38] For the minima, the biggest difference between the UB3LYP and UBMK enthalpies is 2.0 kcal/mol, the products of isomerization having an average difference of 0.4 versus 1.1 kcal/mol for the products of dissociation. In comparison, the differences between the two methods for transition structures are larger with the average for isomerization reactions being 1.2 kcal/mol and that for dissociation reactions being 3.1 kcal/mol. The UBMK energies are universally slightly higher than the UB3LYP energies. The interpretations and overall conclusions reached above are identical irrespective of which DFT method is used.

When comparing the results of this study with the results of O'Hair and co-workers,[21,22,40] it would appear that radical-induced dissociations in peptides are only competitive when the charge is immobilized by attachment of a phosphonium group[21] or sequestered.[22,40] In many respects, there is a strong parallel in charge-remote fragmentations observed in peptides containing a phosphonium fixed charge and enhanced cleavage at acidic residues observed in protonated peptides in which the proton is sequestered on the highly basic residue arginine.[41]

Acknowledgment. We thank Julia Laskin and Richard O'Hair for most helpful discussions. I.K.C. thanks the Research Grant Council, Hong Kong; A.C.H. and K.W.M.S. thank the Natural Sciences and Engineering Research Council, Canada, for financial support. This work was made possible by the facilities of the Shared Hierarchical Academic Research Computing Network (SHARCNET: www.sharcnet.ca).

Supporting Information Available: Tables of coordinates and energies obtained with the UB3LYP and UBMK methods. This material is available free of charge via the Internet at http://pubs.acs.org

JA801108J

(40) Wee, S.; O'Hair, R. A. J.; McFayden, W. D. *Int. J. Mass Spectrom.* **2004**, *234*, 101–122.
(41) Wysocki, V. H.; Tsaprailis, G.; Smith, L. L.; Breci, L. A. *J. Mass Spectrom.* **2000**, *35*, 1399–1406.